# Supporting Information

## Molecularly designed N, S co-doped carbon nanowalls decorated on graphene as highly efficient sulfur reservoir for Li-S batteries: a supramolecular strategy

Jinmeng Sun,[a] Yuhang Liu,[a] Hongfang Du,[a] Song He,[a] Lei Liu,[a] Zhenqian Fu,[a,b] Linghai Xie,[a,c] Wei Ai*[a] and Wei Huang*[a,b,c]

[a]*Institute of Flexible Electronics (IFE), Northwestern Polytechnical University (NPU), 127 West Youyi Road, Xi'an 710072, China*

[b]*Key Laboratory of Flexible Electronics (KLOFE) & Institute of Advanced Materials (IAM), Jiangsu National Synergetic Innovation Center for Advanced Materials (SICAM), Nanjing Tech University (NanjingTech), 30 South Puzhu Road, Nanjing 211816, China*

[c]*Key Laboratory for Organic Electronics & Information Displays (KLOEID) and Institute of Advanced Materials (IAM), SICAM, Nanjing University of Posts & Telecommunications, Nanjing 210023, China*

## Experimental section

### *1. Synthesis of NSCNWs-G and NSCNWs-G/S*

GO was prepared by a modified Hummer's method. 300 mg GO was dispersed in 150 mL distilled water under sonication for 1 h, then 150 mL DMF was added under stirring. Next, 420 mg MEL was dissolved into the solution at 80 ℃, and 19 mg/mL TTCA solution (570 mg TTCA in 30 mL DMF) was dropwise added into the above suspension. Subsequently, the mixture was stirred for 15 h, and the precipitates were collected by filtration, washed with distilled water, and dried at 100 ℃ overnight. The resultant powder was annealed at 800 ℃ for 2 h under Ar atmosphere to get NSCNWs-G (heating rate: 5 ℃/min, gas flow: 100 sccm).

NSCNWs-G/S composite was prepared by melt-diffusion method. In a typical

synthesis, NSCNWs-G and sublimed sulfur were grinded with a mass ratio of 2:8. Afterwards, the mixture was sealed in a stainless-steel autoclave and then subjected to thermal treatment at 155 ℃ for 12 h in an electronic oven. After cooling to room temperature, the NSCNWs-G/S composite was obtained.

## *2. Synthesis of rGO and rGO/S*

rGO was obtained by directly annealing GO at 800 ℃ for 2 h under the same condition with NSCNWs-G. rGO/S was then fabricated via melt-diffusion.

## *3. Experiments of polysulfides adsorption*

20 mg NSCNWs-G and rGO was separately added into the glass vial containing 5 mM $Li_2S_6$ in DME (10 mL), and a same solution without addition of any host materials was set as blank group. After 1 min shaking, the color changes of the solution were pictured. All the procedures were conducted in Ar-filled glove box with $O_2$ and $H_2O$ both below 0.1 ppm. Afterwards, the supernatants derived from the three samples was characterized via UV-vis measurement.

## *4. XPS measurement of $Li_2S_4$ and NSCNWs-G-$Li_2S_4$*

$Li_2S_4$ (0.1 M) solution was first prepared by adding $Li_2S$ and S powder with a stoichiometry ratio of 1:3 into DME. After vigorously stirring for 48 h under 60 ℃ in Ar-filled glove box, the precipitation was completely dissolved. The $Li_2S_4$ powder was obtained via evaporating the solvent in $Li_2S_4$ solution at 60 ℃ in a vacuum oven. For NSCNWs-G-$Li_2S_4$, NSCNWs-G was dispersed in $Li_2S_4$ solution then stirred for 6 h in a glove box. Followed by vacuum drying at 60 ℃, the final sample was collected for XPS measurement.

## *5. Fabrication of symmetric cell for kinetic study*

For symmetric cells assembly, the working electrodes were prepared by casting NSCNWs-G or rGO containing slurry onto an Al foil, in which the slurry is obtained by mixing 80 wt% composite, 10 wt% poly(vinylidene fluoride) (PVDF), and 10 wt% carbon black. After drying in a vacuum oven at 60 ℃ for 12 h, the electrodes were punched into 12 mm diameter disks. Symmetric cells were then assembled using 0.1 M

$Li_2S_6$ dissolved in 1,3-dioxolane (DOL) and 1,2-dimethoxyethane (DME) mixture (1:1 in v:v) as the electrolyte, which also contains 1 M lithium bis(trifluoromethanesulfonyl)imide (LiTFSI) and 0.1 M $LiNO_3$. The cut-off voltage of CV measurements was set as -1 to 1 V under scan rates ranging from 1 to 5 mV $s^{-1}$.

## *6. Experiments of $Li_2S$ nucleation on NSCNWs-G and rGO*

0.25 M $Li_2S_8$ catholyte was prepared by adding $Li_2S$ and S (mole ratio: 1:7) into TEDGME containing 1 M LiTFSI. NSCNWs-G (rGO) was dispersed into ethanol, then dropwise added onto carbon papers (CPs) with diameter of 12 mm. After drying at 60 ℃ overnight, the NSCNWs-G/CPs (rGO/CPs) was obtained and served as the working electrode with 40 μL 0.25 M $Li_2S_8$ catholyte. Lithium metal was employed as encounter electrode with 40 μL electrolyte without $Li_2S_8$ but containing 1% $LiNO_3$. The assembled cell was first subjected to a galvanostatic discharge at 112 mA with a cutoff voltage of 2.06 V, then undergoing potentiostatic discharge at 2.05 V. The current response to discharge time was recorded.

## *7. Materials characterizations*

SEM images were obtained on a scanning electron microscope (FEI Verios G4) at an accelerating voltage of 10 kV. TEM and STEM images were taken with a transmission electron microscope (FEI Talos F200X) with an accelerating voltage of 200 kV. XPS analysis was performed on an ESCALAB MK II X-ray photoelectron spectrometer with a monochromatic Al Kα X-ray source. XRD patterns were recorded on a Shimadzu XRD-7000s diffraction instrument with Cu Kα radiation (λ = 1.54056 Å). Nitrogen adsorption/desorption analysis was performed at 77 K on a TriStar Ⅱ 20 apparatus. TGA was carried out on a NETCSCH T209 apparatus from 25 ℃ to 800 ℃ with a heating rate of 10 ℃ $min^{-1}$ in $N_2$ atmosphere.

## *8. Electrochemical measurements*

For Li-S batteries assembly, the working electrode was fabricated by casting the slurry containing 70 wt% S-based composite (i.e., NSCNWs-G/S and rGO/S), 20 wt% carbon black, and 10 wt% PVDF onto an Al foil. The areal mass loading of active

material was calculated to be 1.2 mg/cm$^2$. Li foil and Celgard 2400 polypropylene membrane were used as the counter electrode and separator, respectively. 1 M LiTFSI and 0.1 M $LiNO_3$ dissolved in DOL and DME mixture was used as the electrolyte. Electrochemical performances were measured with a NEWARE battery analyzer and a CHI 760D electrochemical workstation.

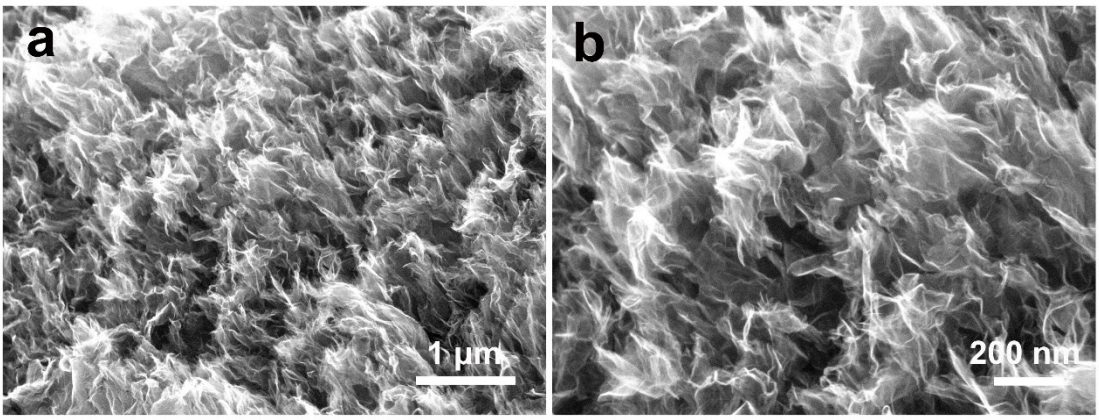


**Fig. S1** (a, b) SEM images of the lateral side of NSCNWs-G with different magnifications.

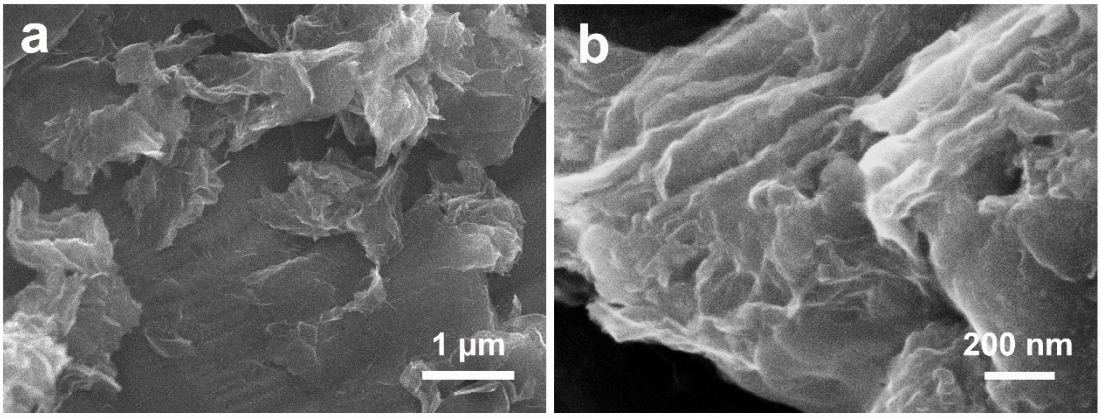


**Fig. S2** (a, b) SEM images of rGO with different magnifications.

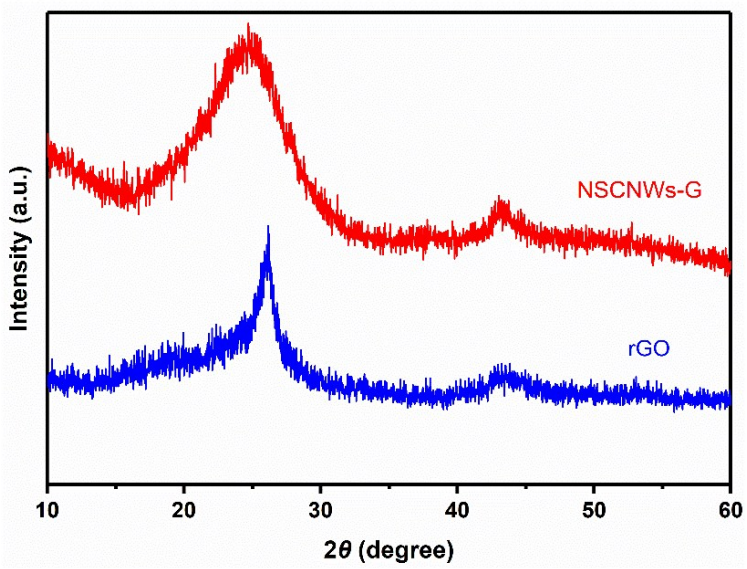


**Fig. S3** XRD patterns of NSCNWs-G and rGO.

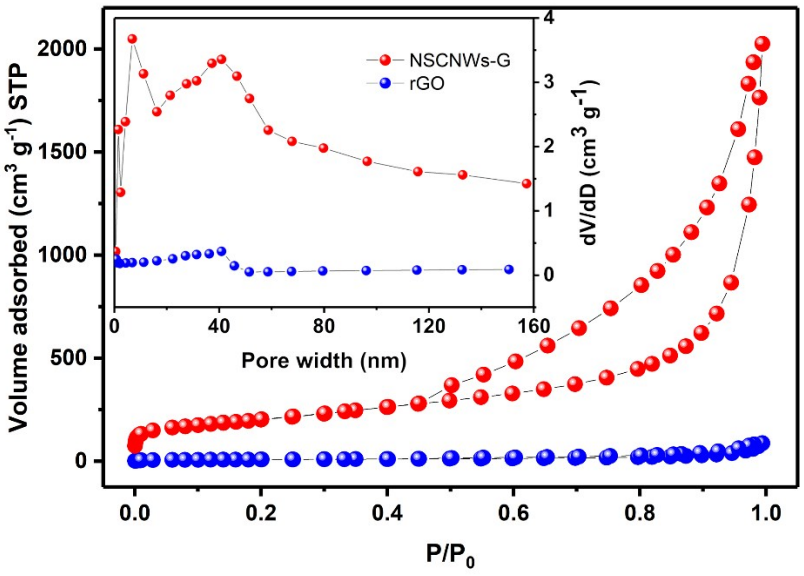


**Fig. S4** $N_2$ adsorption/desorption isotherms of NSCNWs-G and rGO. The inset is the corresponding pore size distribution plots.

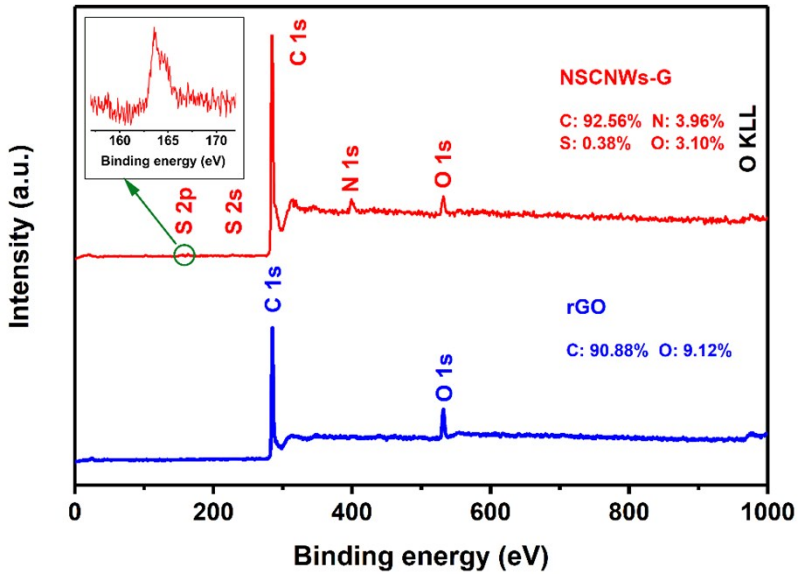


**Fig. S5** XPS survey spectra of NSCNWs-G and rGO.

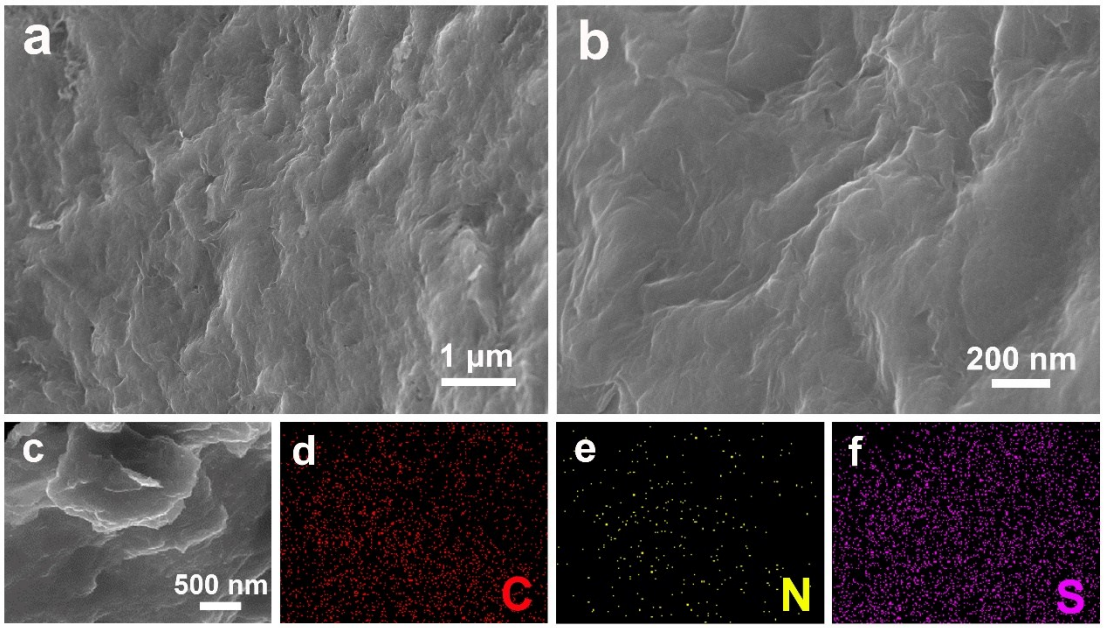


**Fig. S6** (a, b) SEM images of NSCNWs-G/S composite with different magnifications. (c-f) EDS mapping images of NSCNWs-G/S.

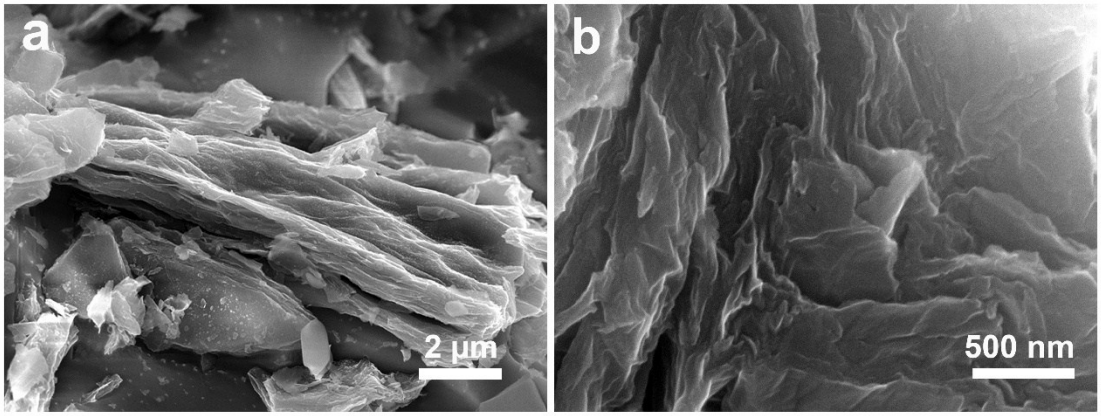


**Fig. S7** (a and b) SEM images of rGO/S composite with different magnifications.

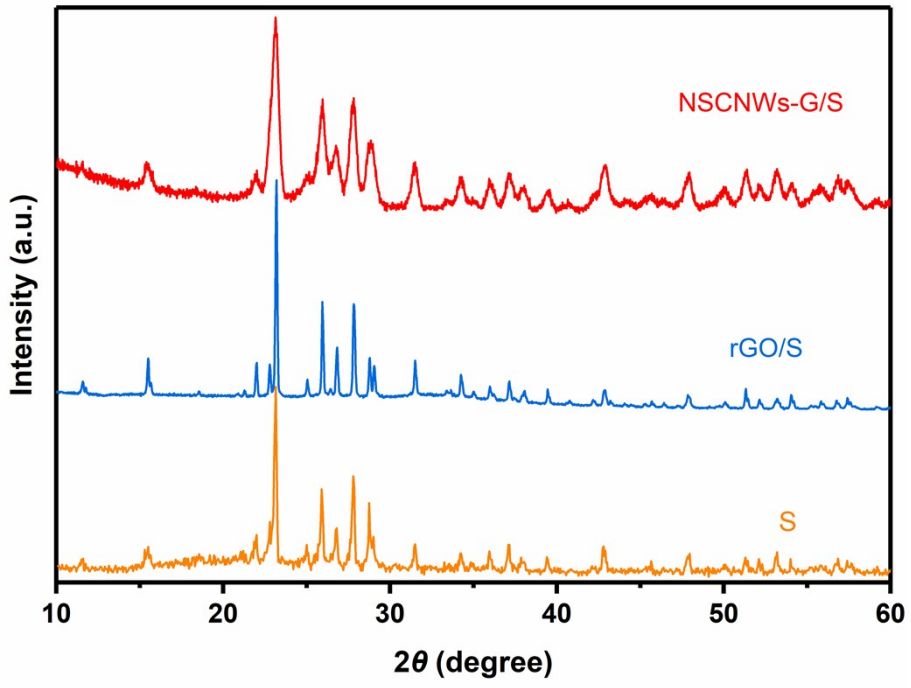


**Fig. S8** XRD patterns of NSCNWs-G/S, rGO/S and sulfur.

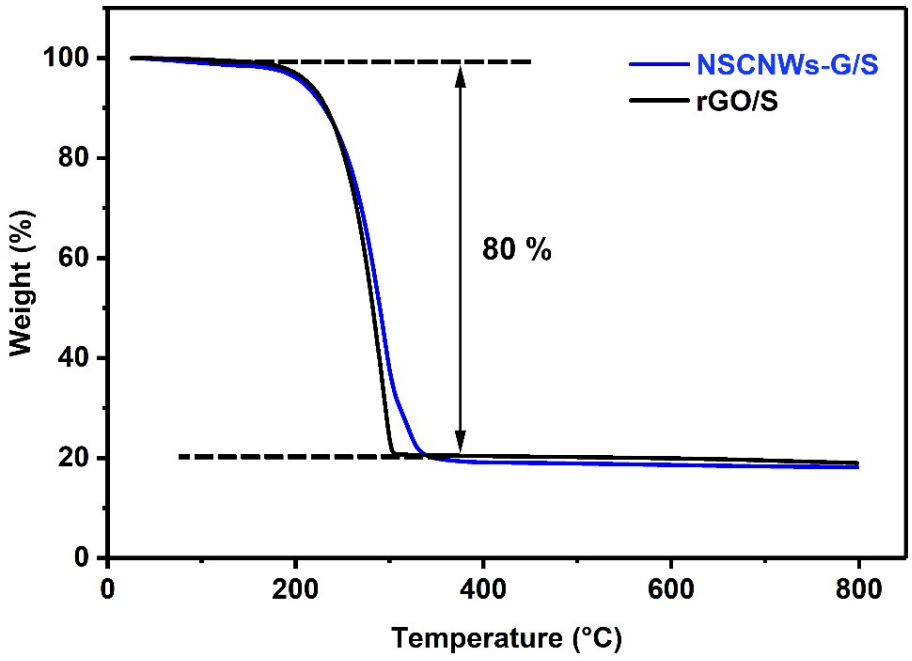


**Fig. S9** TGA profiles of NSCNWs-G/S and rGO/S composites.

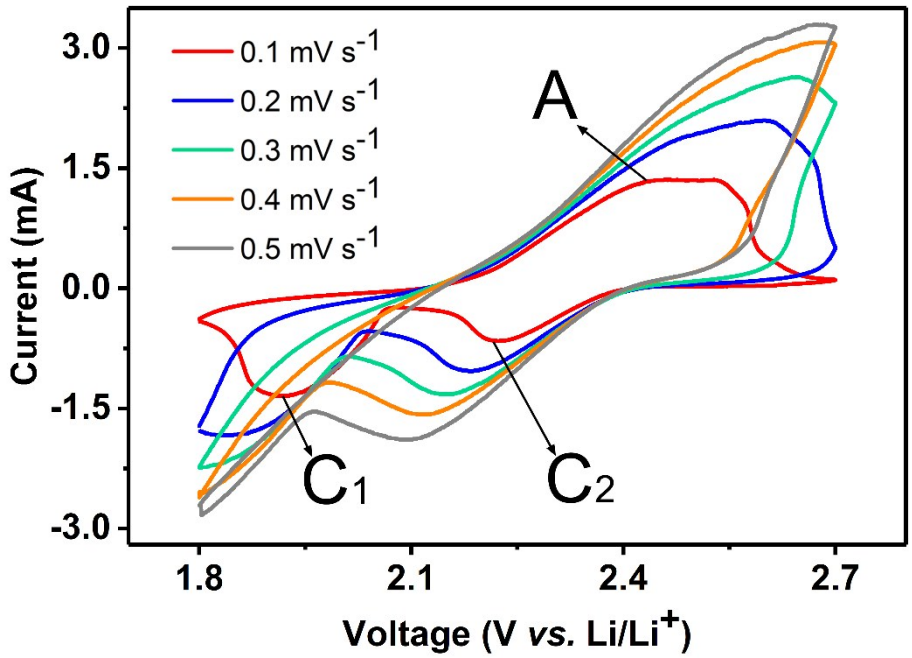


**Fig. S10** CV profiles of rGO/S cathode at different scan rates.

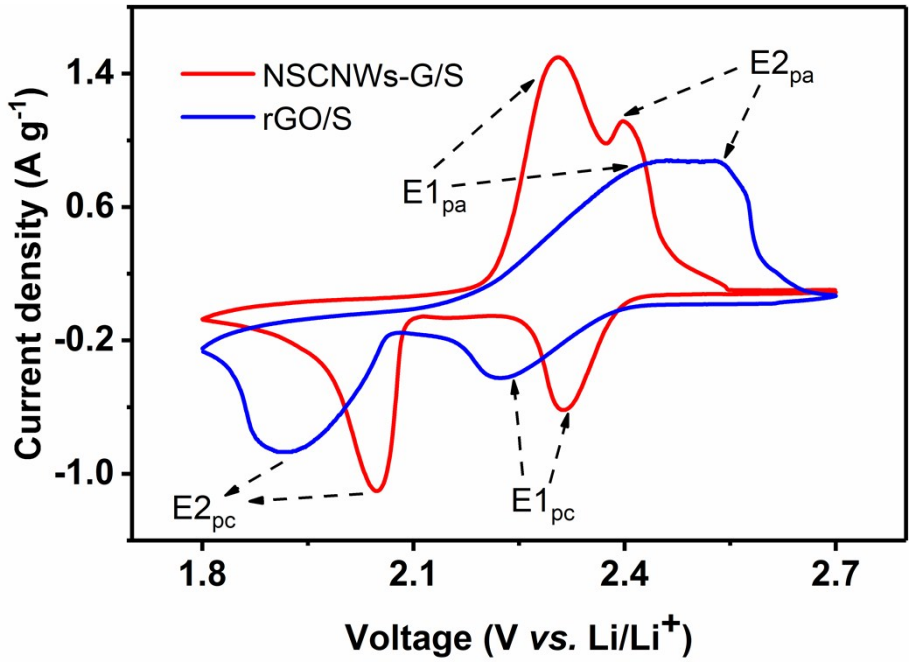


**Fig. S11** CV profiles of NSCNWs-G/S and rGO/S cathode at a scan rate of 0.1 mV $s^{-1}$.

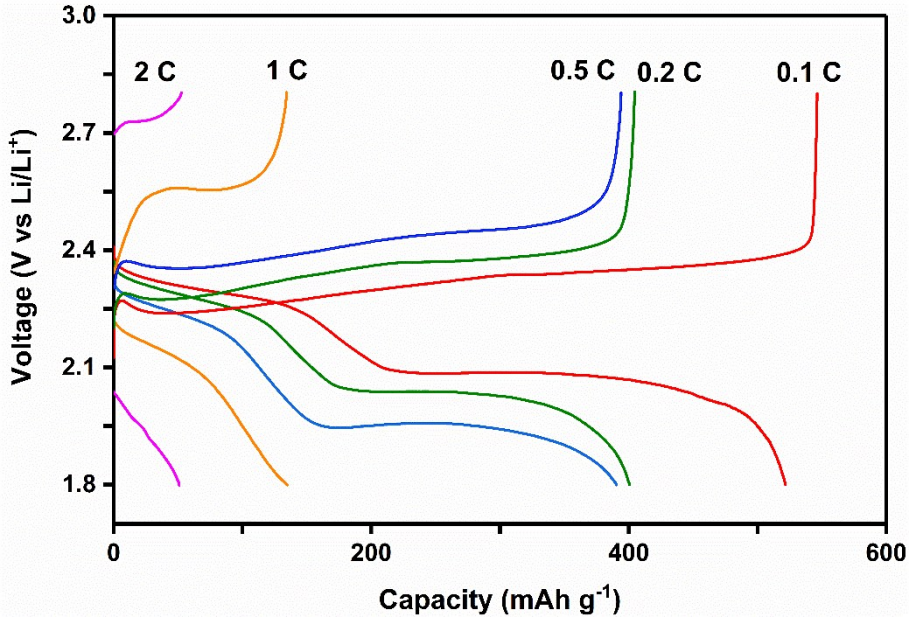


**Fig. S12** Typical discharge/charge voltage profiles of rGO/S cathodes at different current rates.

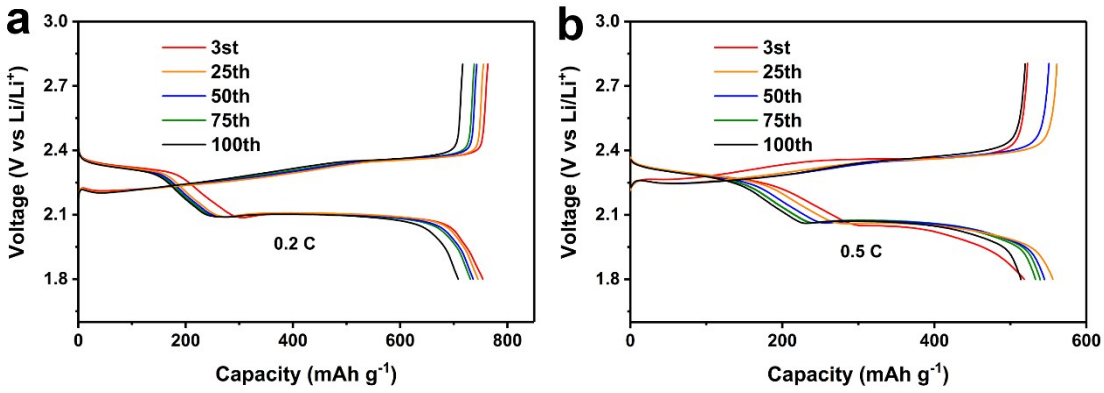


**Fig. S13** Galvanostatic profiles of NSCNWs-G/S at (a) 0.2 C and (b) 0.5 C at different cycles.

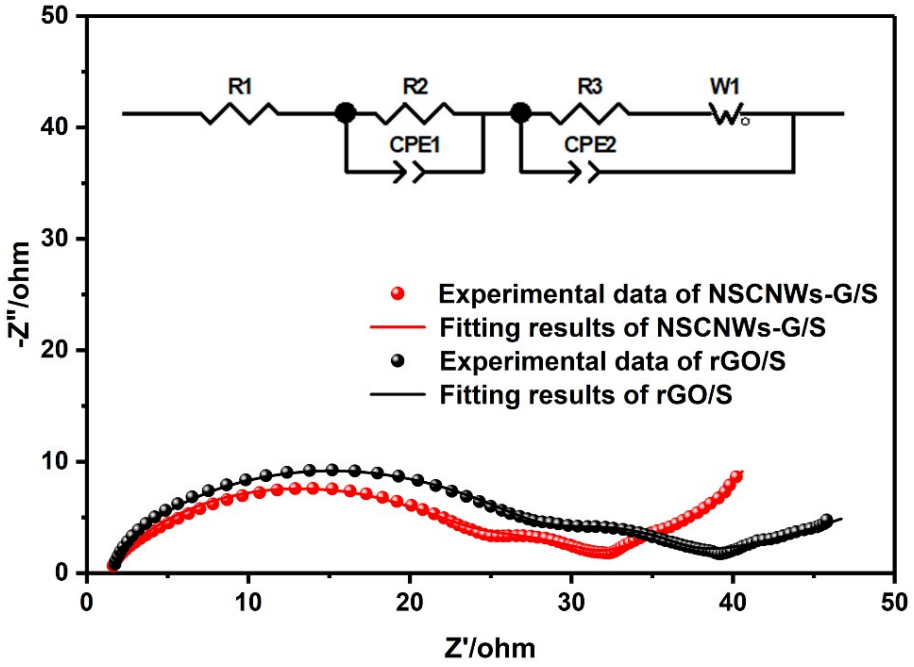


**Fig. S14** Nyquist plots of NSCNWs-G/S and rGO/S cathodes.

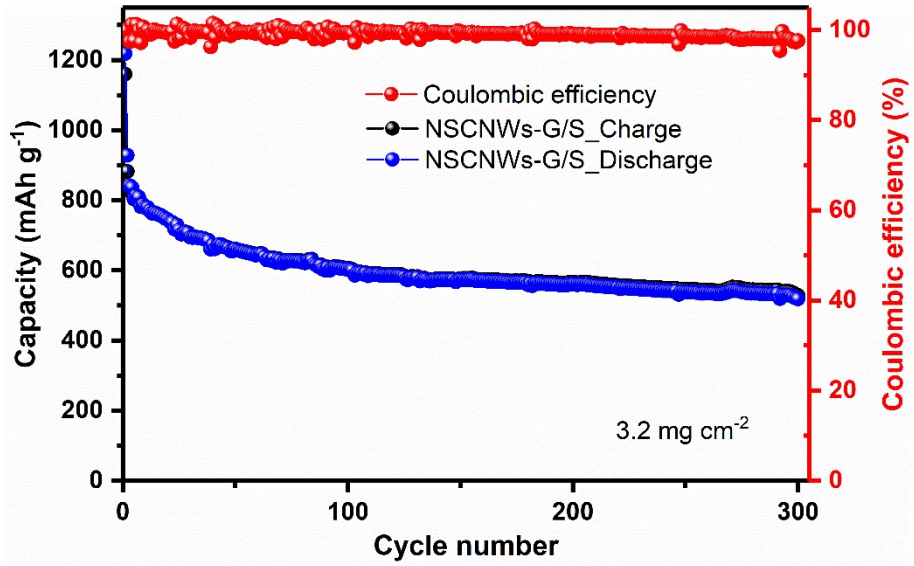


**Fig. S15** Cycling performance of NSCNWs-G/S at 0.5 C with high sulfur areal loading.

**Table S1.** Electrochemical parameters of NSCNWs-G/S and rGO/S derived from their cyclic voltammograms at a scan rate of 0.1 mV $s^{-1}$.

| Samples | $E1_{pa}$, $E2_{pa}$ (V) | $E1_{pc}$, $E2_{pc}$ (V) | Difference value: $E1_{pa}$, $E1_{pc}$ (V) | Exchange current density ($I_{0,a}$ $I_{0,c}$) (mA $cm^{-2}$) |
|---|---|---|---|---|
| NSCNWs-G/S | 2.304, 2.397 | 2.317, 2.049 | 0.013 | 1.08, 1.29 |
| rGO | 2.431, 2.532 | 2.229, 1.918 | 0.202 | 1.04, 1.07 |

**Table S2.** Performance comparison between this work and other related works in terms of the capacity decay rate.

| Sample | Capacity decay with areal loading of 1~2 mg $cm^{-2}$ | Ref. |
|---|---|---|
| S/Co-CNCs | 0.19% at 0.5 C for 180 cycles, 0.029 at 2 C for 600 cycles | S1 |
| Co, N-CNTs-CNS/CFC | 0.069% at 0.5 C for 250 cycles | S2 |
| S@Co/N-PCNSs | 0.26% at 0.2 C for 100 cycles, 0.036% at 5 C for 400 cycles | S3 |
| S-NPC/G | 0.043% at 1 C for 300 cycles | S4 |
| HCMs-S | 0.04% at 1(2) C for 900 cycles | S5 |
| HNPC-900-65S | 0.10% at 0.5 C for 400 cycles, 0.035% at 2 C for 800 cycles | S6 |
| S@HPTCF | 0.30% at 0.2 C for 50 cycles | S7 |
| Fe-PGM-S | 0.09% at 2 C for 500 cycles, 0.08% at 5 C for 1000 cycles | S8 |
| S/CC@$Co_9S_8$-$Co_4N$ | 0.027% at 1 C for 1000 cycles | S9 |
| CNT@$TiO_{2-x}$-S | 0.33% at 0.2 C for 100 cycles, 0.059% at 1 C for 500 cycles | S10 |
| $Fe_2O_3$@N-PC/$Mn_3O_4$-S | 0.052% at 0.5 C for 200 cycles | S11 |
| S-NC@$MoS_2$ | 0.2% at 0.5 C for 100 cycles, 0.15% at 1C for 150 cycles, 0.049% at 2C for 1000 cycles | S12 |
| GA-DR-$MoS_2$/S | 0.085% at 0.2 C for 500 cycles, 0.042% at 2 C for 500 cycles | S13 |
| CoSP/rGO/S | 0.13% at 0.5 C for 200 cycles, 0.046% at 1 C for 900 cycles | S14 |
| $Bi_2S_3$–PPy/S | 0.076% at 1C for 500 cycles | S15 |
| CoS2@NGCNs/S | 0.075% at 1C for 300 cycles | S16 |
| Ni-Fe-P/NC/S | 0.087% at 1C for 300 cycles | S17 |
| S@$Ni_3(HITP)_2$-CNT | 0.32% at 0.2 C for 100 cycles, 0.11% at 0.5 C for 150 cycles, 0.116% at 1 C for 300 cycles | S18 |
| $MoS_{2-x}$/rGO/S | 0.083% at 0.5 C for 600 cycles | S19 |
| S@RGO-$CoSe_2$ | 0.071% at 1 C for 400 cycles | S20 |
| A-3DNG/S | 0.11% at 0.2 C for 200 cycles, 0.052% at 1 C for 200 cycles | S21 |
| NSCNWs-G/S | 0.078% at 0.2 C for 100 cycles, 0.021% at 0.5 C for 800 cycles | This work |

## References


S1. Q. Wu, X. Zhou, J. Xu, F. Cao and C. Li, *ACS Nano*, 2019, **13**, 9520-9532.

S2. D. Fang, Y. Wang, C. Qian, X. Liu, X. Wang, S. Chen and S. Zhang, *Adv. Funct. Mater.*, 2019, **29**, 1900875.

S3. S. Liu, J. Li, X. Yan, Q. Su, Y. Lu, J. Qiu, Z. Wang, X. Lin, J. Huang, R. Liu, B. Zheng, L. Chen, R. Fu and D. Wu, *Adv. Mater.*, 2018, **30**, e1706895.

S4. K. Chen, Z. Sun, R. Fang, Y. Shi, H.-M. Cheng and F. Li, *Adv. Funct. Mater.*, 2018, **28**, 1707592.

S5. X. Zhou, J. Tian, Q. Wu, J. Hu and C. Li, *Energy Storage Mater.*, 2019, DOI: 10.1016/j.ensm.2019.06.009.

S6. Z. Li, Z. Xiao, S. Wang, Z. Cheng, P. Li and R. Wang, *Adv. Funct. Mater.*, 2019, **29**, 1902322.

S7. W. Cai, G. Li, D. Luo, G. Xiao, S. Zhu, Y. Zhao, Z. Chen, Y. Zhu and Y. Qian, *Adv. Energy Mater.*, 2018, **8**, 1802561.

S8. C. Zheng, S. Niu, W. Lv, G. Zhou, J. Li, S. Fan, Y. Deng, Z. Pan, B. Li, F. Kang and Q.-H. Yang, *Nano Energy*, 2017, **33**, 306-312.

S9. H. Zhang, Z. Zhao, Y.-N. Hou, Y. Tang, J. Liang, X. Liu, Z. Zhang, X. Wang and J. Qiu, *J. Mater. Chem. A*, 2019, **7**, 9230-9240.

S10. Y. Wang, R. Zhang, J. Chen, H. Wu, S. Lu, K. Wang, H. Li, C. J. Harris, K. Xi, R. V. Kumar and S. Ding, *Adv. Energy Mater.*, 2019, **9**, 1900953.

S11. H. Liu, Z. Chen, L. Zhou, K. Pei, P. Xu, L. Xin, Q. Zeng, J. Zhang, R. Wu, F. Fang, R. Che and D. Sun, *Adv. Energy Mater.*, 2019, DOI: 10.1002/aenm.201901667.

S12. S. Li, Z. Han, W. Hu, L. Peng, J. Yang, L. Wang, Y. Zhang, B. Shan and J. Xie, *Nano Energy*, 2019, **60**, 153-161.

S13. M. Liu, C. Zhang, J. Su, X. Chen, T. Ma, T. Huang and A. Yu, *ACS Appl. Mater. Interfaces*, 2019, **11**, 20788-20795.

S14. X. Chen, X. Ding, H. Muheiyati, Z. Feng, L. Xu, W. Ge and Y. Qian, *Nano Res.*, 2019, **12**, 1115-1120.

S15. B. Long, Z. Qiao, J. Zhang, S. Zhang, M.-S. Balogun, J. Lu, S. Song and Y. Tong, *J. Mater. Chem. A*, 2019, **7**, 11370-11378.

S16. S. D. Seo, D. Park, S. Park and D. W. Kim, *Adv. Funct. Mater.*, 2019, **29**, 1903712.

S17. X. Chen, S. Zeng, H. Muheiyati, Y. Zhai, C. Li, X. Ding, L. Wang, D. Wang, L. Xu, Y. He and Y. Qian, *ACS Energy Lett.*, 2019, **4**, 1496-1504.

S18. D. Cai, M. Lu, Li, J. Cao, D. Chen, H. Tu, J. Li and W. Han, *Small*, 2019, **15**, e1902605.

S19. H. Lin, L. Yang, X. Jiang, G. Li, T. Zhang, Q. Yao, G. W. Zheng and J. Y. Lee, *Energy Environ. Sci.*, 2017, **10**, 1476-1486.

S20. L. Chen, W. Yang, J. Liu and Y. Zhou, *Nano Res.*, 2019, **12**, 2743-2748.

S21. A. Benítez, A. Caballero, J. Morales, J. Hassoun, E. Rodríguez-Castellón and J. Canales-Vázquez, *Nano Res.*, 2019, **12**, 759-766.